

Observation of Single Dirac Cone Topological Surface State in Compounds TlBiTe_2 and TlBiSe_2 from a New Topological Insulator Family

Yulin Chen,^{1,2,3} Zhongkai Liu,^{1,2} James G. Analytis,^{1,2} Jiun-Haw Chu,^{1,2} Haijun Zhang,^{1,2} Sung-Kwan Mo,³ Robert G. Moore,¹ Donghui Lu,^{1,2} Ian Fisher,^{1,2} Shoucheng Zhang,^{1,2} Zahid Hussain,³ and Z.-X. Shen^{1,2}

¹Stanford Institute for Materials and Energy Sciences,

SLAC National Accelerator Laboratory, 2575 Sand Hill Road, Menlo Park, California 94025

²Geballe Laboratory for Advanced Materials, Departments of Physics and Applied Physics, Stanford University, Stanford, California 94305

³Advanced Light Source, Lawrence Berkeley National Laboratory Berkeley California, 94720, USA

(Dated: October 30, 2018)

Angle resolved photoemission spectroscopy (ARPES) studies were performed on two compounds (TlBiTe_2 and TlBiSe_2) from a recently proposed three dimensional topological insulator family in Thallium-based III-V-VI₂ ternary chalcogenides. For both materials, we show that the electronic band structures are in broad agreement with the *ab initio* calculations; by surveying over the entire surface Brillouin zone (BZ), we demonstrate that there is a single Dirac cone reside at the center of BZ, indicating its topological non-triviality. For TlBiSe_2 , the observed Dirac point resides at the top of the bulk valance band, making it a large gap ($\geq 200\text{meV}$) topological insulator; while for TlBiTe_2 , we found there exist a negative indirect gap between the bulk conduction band at M point and the bulk valance band near Γ , making it a semi-metal at proper doping. Interestingly, the unique band structures of TlBiTe_2 we observed further suggest TlBiTe_2 may be a candidate for topological superconductors.

PACS numbers: 71.18.+y, 71.20.-b, 73.20.-At, 73.23.-b

Topological insulators represent a new state of quantum matter with a bulk gap and odd number of relativistic Dirac fermions on the surface [1]. Since the discovery of two dimensional (2D) topological insulator in HgTe quantum well [2, 3] and subsequent in three dimensional (3D) materials (especially the single Dirac cone family Bi_2Te_3 , Bi_2Se_3 and Sb_2Te_3)[4–6], topological insulators has grown as one of the most intensively studied fields in condensed matter physics [1–11]. The massless Dirac fermions and the magnetism further link the topological insulators to relativity and high energy physics [12]. The fast development of the topological insulators also inspires the study of other topological states such as topological superconductors [13–19], which has a pairing gap in the bulk and topologically protected surface state consisting of Majorana fermions [13]. Unlike Dirac fermions in topological insulators that can have the form of particles or holes, Majorana fermions are their own antiparticles [20]. The simplest 3D topological superconductor consists of a single Majorana cone on the surface, containing half the degree of freedom of the Dirac surface state of a single cone 3D topological insulator. This fractionalization of the degree of freedom introduces quantum non-locality and is essential to the topological quantum computing based on Majorana fermions [21].

In this work, we use ARPES to study the electronic structure of TlBiTe_2 and TlBiSe_2 from a recently proposed topological insulator family: Thallium-based III-V-VI₂ ternary chalcogenides [22, 23]. Remarkably, both the surface and bulk electronic structures are in broad agreement with the *ab initio* calculations; and a single

Dirac cone centered at the Γ point of surface Brillouin zone is found in both materials. Furthermore, for the p-type TlBiTe_2 , the experimental band structure shows six leaf-like bulk valance band pockets around the Dirac cone. Given that these leaf-like bulk pockets are the only structure other than the surface Dirac cone on the Fermi-surface (FS), they may provide a possible origin of the reported bulk superconductivity [24], which can further induce superconductivity on the surface state by proximity effect, making TlBiTe_2 a candidate for 3D topological superconductors. Another compound of the family, TlBiSe_2 has a simpler bulk structure around the single Dirac cone at the Γ point, with the Dirac point resides on top of the the bulk energy gap ($\sim 200\text{meV}$), making it a large gap topological insulator similar to Bi_2Se_3 [4], but with better mechanical properties than the $\text{Bi}_2\text{Se}_3/\text{Bi}_2\text{Te}_3$ family, as the bonding between layers are much stronger [22] than the van de Waals' force that bonds quintuple layer units of Bi_2Te_3 or Bi_2Se_3 [4].

The crystal structure of Thallium based III-V-VI₂ ternary chalcogenides is rhombohedra with the space group R-3m, which can be viewed as a distorted NaCl structure with four atoms in the primitive unit cell. A conventional unit cell of TlBiTe_2 is shown in Fig. 1(a) as an example: the three different types of atoms stack in layers with repeating sequence ...-Te-Bi-Te-Tl...[25]. The existence of a flat cleavage plane [26] parallel to the (111) surface in this family of compounds [inset of Fig. 1(b)] makes them suitable for ARPES study. The high quality of the crystal was demonstrated by the XRD [Fig. 1(b)] and Laue [Fig 1(c)] characterizations; and the

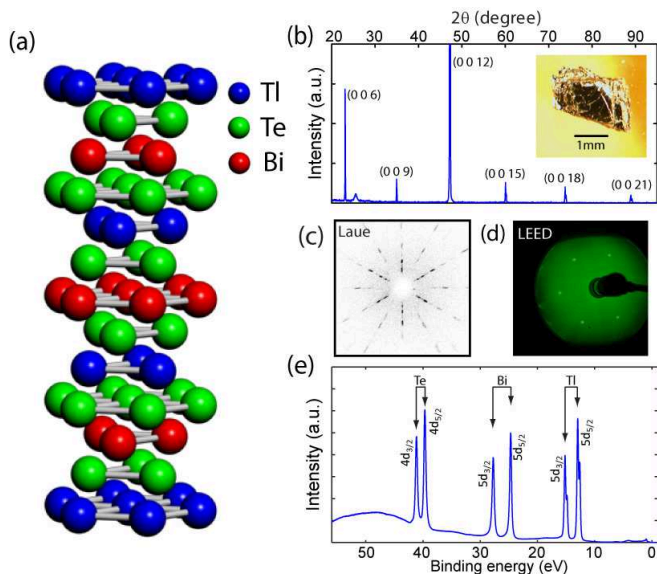


FIG. 1: (color) (a) Crystal structure of TlBiTe_2 with repeating layers -Tl-Te-Bi-Te-. (b) XRD study on the as grown crystal shows clean characteristic peaks. The photo of a sample in inset shows mirror-like cleavage plane parallel to the (111) plane. (c) Sharp Laue pattern confirms the high quality of the crystals used for ARPES measurements. (d) LEED pattern on a cleaved surface after ARPES measurement demonstrates clear surface diffraction spots without surface reconstruction. (e) Core level PES demonstrates the characteristic peaks from d-shell electrons of all three compositional elements.

LEED pattern on the sample surface after ARPES measurement (Fig. 1d) confirmed that the surface structure of the samples is free from reconstruction. The characteristic peaks of all three elements can be identified in core level photoemission measurements [Fig.1(e)].

Figure 2 displays TlBiTe_2 band structure around the center of the BZ. The 3D band structure [Fig.2(a)] shows a clear Dirac cone centered at the Γ -point with broad features from bulk conduction (BCB) and bulk valence band (BVB) as theoretically predicted [22, 23]. To confirm the surface nature of the Dirac cone, excitation photon energy dependent ARPES study (Fig.2b) was performed. The non-varying shape of the outer hexagonal surface state band (SSB) FS with different excitation photon energies indicates its 2D nature; while the shape and the existence of the BCB FS pocket inside changes dramatically due to its 3D nature with strong k_z dispersion as expected.

Detailed band dispersions along two high symmetry directions ($\Gamma - M$ and $\Gamma - K$) are illustrated in Fig. 2(c), in which an asymmetry of the BVB along the two directions can be seen. Based on the characteristic energy positions of the bulk band, we can divide the band structure into four regions [Fig. 2(c)] for discussion of different FS geometries [Fig. 2(d)]. From region I to III, the bulk contribution of the FS evolves from an n-type pocket in-

side (region I) the n-type SSB FS to six p-type leaf-like pockets outside (Region III), with the bulk pockets disappear in region II; while in region IV, both the FS at the center and the surrounding leaf-like pockets are p-type. Fig. 2(e) shows a summary of the band evolution through all four regions.

Besides having the single Dirac cone on the surface, TlBiTe_2 was also reported to superconduct when p-doped [24], with E_F of the corresponding density ($\sim 6 \times 10^{20}/\text{cm}^3$) resides in region III (about 150meV below the bottom of BVB). From our measurements, the FS geometry in this region is characterized by a ring like SSB FS and six surrounding p-type bulk pockets [Fig. 3(a)], as clearly shown in Fig. 2(d) - where a broad scan in k -space that covers four BZs [Fig. 3(b)] confirms that the FS structure in Fig. 3(a) is the only feature within each BZ. This leads to the natural conclusion that the bulk superconductivity of p-type TlBiTe_2 originates from the six leaf-like bulk pockets; and in the superconducting state, the surface state [the center FS pocket in Fig. 3(a,b)] can become superconducting due to the proximity effect induced by the bulk states. For such a superconductor, it has been proposed [13] that each vortex line has two Majorana zero modes related by the time reversal symmetry, thus making it a candidate for topological superconductors and suitable for the topological quantum computation [21]. However, the presence of superconductivity in p-type TlBiTe_2 requires further confirmation [27, 28].

The band structures of TlBiTe_2 in larger energy and momentum scale are shown in Fig. 3(c), where the measured dispersions (left sub-panels) along both $\Gamma - M - \Gamma$ and $\Gamma - K - \Gamma$ directions are compared with the corresponding *ab initio* calculation of the bulk band (right sub-panels). In general, the experimental dispersions along both directions agree well with the calculation, which reproduces each bulk feature of the measurement [Fig. 3(c)], albeit the relative energy position is slightly different. Again, the non-existence of the linear dispersion of the Dirac cone in the *ab initio* bulk calculation confirms its surface nature.

Interestingly, from the measurements [Fig. 3(c), top left panel], we find there is a small energy overlap ($\sim 20\text{meV}$) between the bottom of the electron pocket at M (BCB2) and the top of the valence band around Γ (BVB1), indicating that TlBiTe_2 is a semi-metal if E_F resides in this region. Also, unlike the p-type sample, the FS of an n-type TlBiTe_2 (electron density $\sim 10^{19}/\text{cm}^3$) shows an electron pocket at the M point [Fig. 3(d)] due to the bulk conduction band (BCB2) at the zone boundary [Fig. 3(c), top row].

The band structure of TlBiSe_2 , another compound from the Tl-based ternary family, is summarized in Fig. 4. Similar to TlBiTe_2 , there exists a single surface Dirac cone at the Γ point [Fig. 4(a-f)], confirming that its topological non-triviality. The main difference between TlBiSe_2 and TlBiTe_2 is that the Dirac point of TlBiSe_2

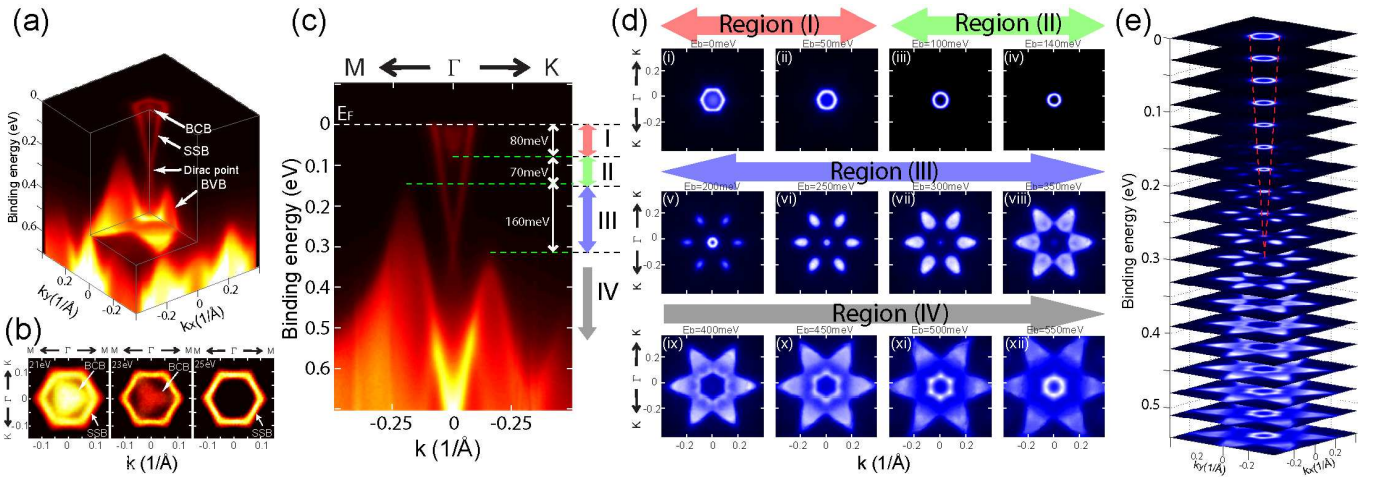


FIG. 2: (Color) (a) 3D representation of the dispersion, with the bulk conduction band (BCB), bulk valance band (BVB) surface state band (SSB) and the Dirac point indicated. (b) Photon energy dependent FS maps (symmetrized according to the crystal symmetry) shows different BCB pockets for 21, 23 and 25eV photons. (c) Band dispersions along the M- Γ -K direction. Four regions defined by characteristic energy positions of the band structure are labeled. (d) Constant energy plot of the band structure in different regions defined in (c), showing the BCB FS inside SSB (region I), SSB only (region II), BVB outside SSB (region III) and all BVB (region IV). (e) Stacking constant energy plots illustrates the evolution of the band structure in different regions. Red dashed line traces the dispersion of the SSB from the Dirac point.

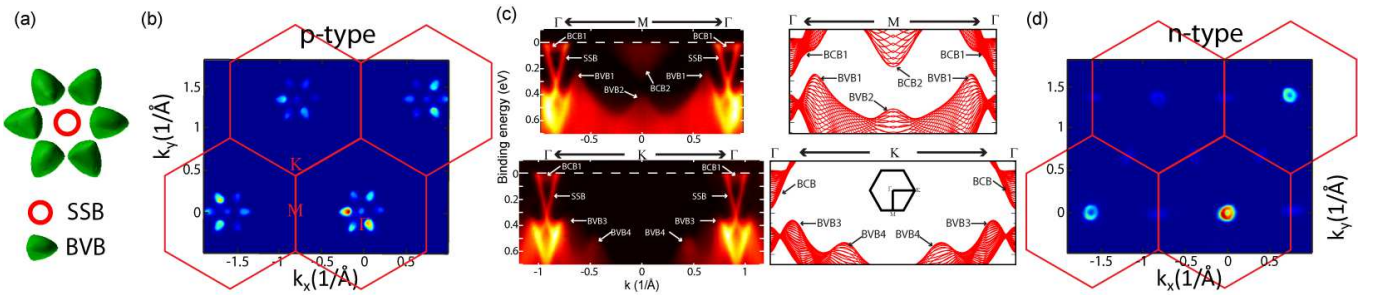


FIG. 3: (Color) (a) Illustration of the typical FS in region III as defined in Fig. 2. The SSB pocket at Γ is surrounded by six leaf-like BVB FS pockets. (b) Broad k -space scan covers four BZs shows no additional features besides the FS pockets illustrated in (a), with the Γ , M and K points marked. (c) Comparison between the measured band structure (left sub panels) and *ab initio* calculations (right sub-panels). Results of $\Gamma - M - \Gamma$ ($\Gamma - K - \Gamma$) direction are shown on the top (bottom) row. Prominent BCB, BVB and SSB features are marked in both measured and calculated band structures. (d) Broad FS map of the n-type sample shows additional BCB pockets at M point in addition to the ring-like SSB pocket around Γ , as a result from the BCB2 band in panel (c) (top row).

resides at the top of the BVB [Fig. 4(a,b)], and the system has a $\sim 200\text{meV}$ direct bulk gap at Γ . The bulk band structure is also simpler around Γ and less anisotropic along Γ -M and Γ -K directions [Fig. 4(a,b)]. This simplicity is also shown in the constant energy contour plots [Fig. 4(c)] and its evolution [Fig. 4(d)]. Comparing Fig. 4(c) and Fig. 2(b), we notice that the SSB FS of TlBiSe₂ is a convex hexagon, contrast to that of TlBiTe₂ which shows slightly concave geometry. This difference resembles the difference between the SSB FSs of Bi₂Te₃ and Bi₂Se₃, and can be reflected by different observations in experiments such as scanning tunneling microscopy/spectroscopy STM/STS [29, 30].

Besides the simpler band geometry around Γ , the

broad range FS map [Fig. 4(e)] of n-type TlBiSe₂ is also simpler than that of the TlBiTe₂ [Fig. 3(d)], without the electron pocket at the M point. This simplicity can also be seen in the band dispersions in Fig. 4(f), where although the experimental (left sub-panels) and calculated (right sub-panels) bulk band structure again show agreement in general, the BCB2 feature at M in the calculation (top right panel) was not seen in the measurements (top left panel), causing the missing of an electron pocket at M in Fig. 4e.

Acknowledgements We thank X. L. Qi, B.H. Yan and C.X. Liu for insightful discussions. This work is supported by the Department of Energy, Office of Basic Energy Science under contract DE-AC02-76SF00515.

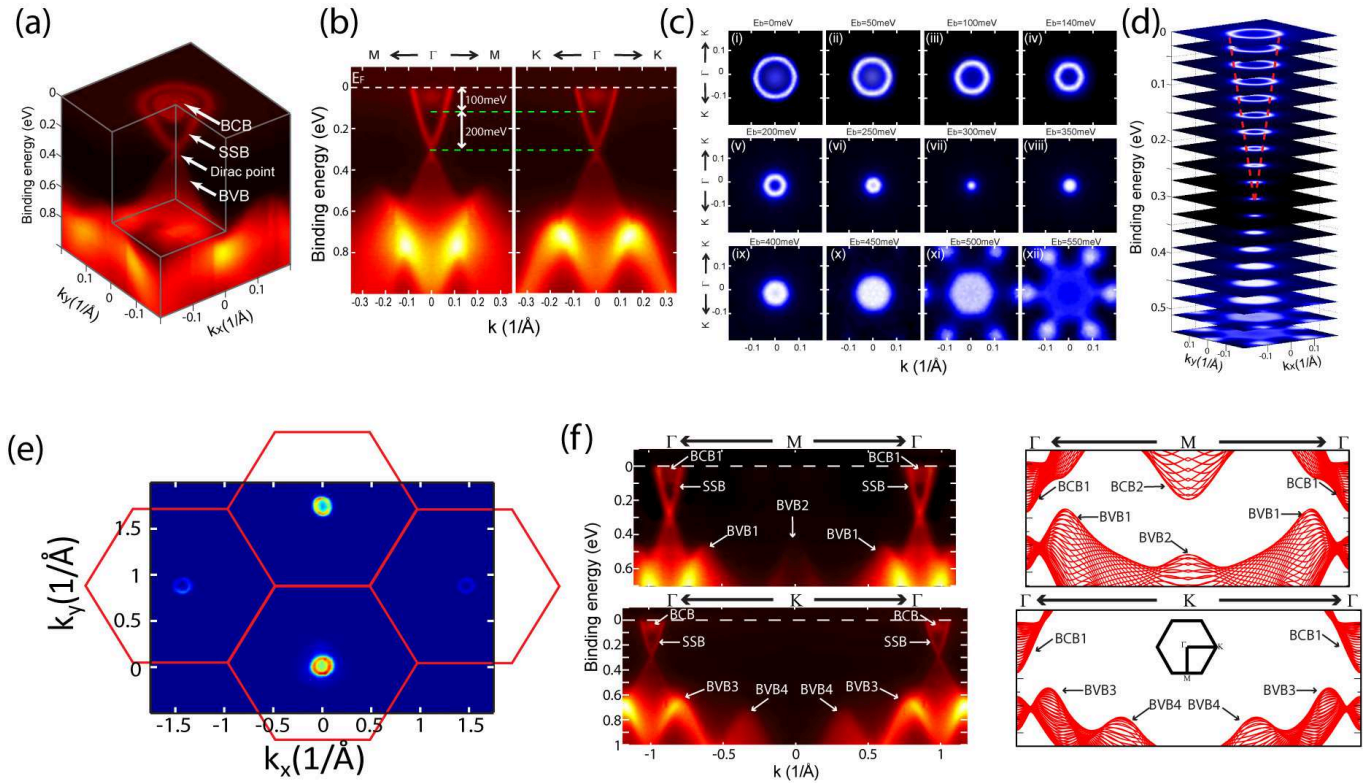


FIG. 4: (Color) (a) 3D illustration of the band structure around Γ , with the BCB, BVB, SSB and the Dirac point indicated. (b) Detailed band structure along $M-\Gamma-K$ direction, with less anisotropy compared to Fig. 2(c). The bottom of the BCB at Γ is about 100meV below E_F and the Dirac point, residing on top of the BVB, is about 200meV below the BCB bottom. (c) Constant energy contours of the band structure at different binding energies. (d) Stacking constant energy plots shows the evolution of the band structure. Red dashed line traces the dispersion of the SSB from the Dirac point. (e) Broad FS map of n-type TlBiSe_2 shows a FS sheet without BCB pocket at M point. (f) Comparison between the measured band structure (left sub panels) and calculations (right sub-panels). Results of $\Gamma - M - \Gamma$ ($\Gamma - K - \Gamma$) direction are shown on the top (bottom) row. Prominent BCB, BVB and SSB features are marked in both the measured and calculated band structures.

[1] X. L. Qi and S. C. Zhang, Phys. Today 63, 33 (2010)
 [2] A. Bernevig, T. L. Hughes and S. C. Zhang, Science 314, 1757 (2006)
 [3] M. Konig et al., Science 318, 766 (2007)
 [4] H. Zhang, et al., Nature Phys. 5, 438 (2009).
 [5] Y. Xia, et al., Nature Phys. 5, 398 (2009).
 [6] Y. L. Chen, et al., Science 325 178 (2009)
 [7] L. Fu, C. L. Kane and E. J. Mele, Phys. Rev. Lett. 98, 106803 (2007)
 [8] X. L. Qi, T. L. Hughes and S. C. Zhang, Phys. Rev. B 78, 195424 (2008)
 [9] J. E. Moore and L. Balents, Phys. Rev. B 75, 121306(R) (2007).
 [10] R. Roy, Phys. Rev. B 79, 195321 (2009)
 [11] B. Seradjeh, J. E. Moore and M. Franz, Phys. Rev. Lett, 103, 066402 (2009)
 [12] F. Wilczek, Nature, 458, 129 (2009)
 [13] X. L. Qi, T. L. Hughes, S. Raghu and S. C. Zhang, Phys. Rev. Lett. 102, 187001 (2009).
 [14] X. L. Qi, T. L. Hughes, and S. C. Zhang, Phys. Rev. B 81, 134508 (2010).
 [15] A. P. Schnyder, S. Ryu, A. Furusaki and A. W. W. Ludwig,

Phys. Rev. B 78, 195125 (2008).
 [16] A. Kitaev, <http://arxiv.org/abs/0901.2686> (2009)
 [17] R. Roy, <http://arxiv.org/abs/0803.2868> (2008).
 [18] L. Fu and C. L. Kane, Phys. Rev. Lett. 100, 096407 (2008).
 [19] Y. S. Hor, J. G. Checkelsky, D. Qu, N. P. Ong and R. J. Cava, <http://arxiv.org/abs/1006.0317> (2010)
 [20] F. Wilczek, Nature Phys. 5, 614-618 (2009).
 [21] C. Nayak, S. H. Simon, A. Stern, M. Freedman and S. D. Sarma, Rev. Mod. Phys. 80, 1083 (2008).
 [22] B. Yan, et. al., Euro. Phys. Lett. 90 37002 (2010)
 [23] H. Lin, et. al., <http://arxiv.org/abs/1003.2615>
 [24] R. Hein and E. Swiggard, Phys. Rev. Lett. 24, 53-55 (1970).
 [25] E. F. Hockings and J. G. White, Acta Crystallographica 14, 328 (1961).
 [26] M. Ozer, K. M. Paraskevopoulos, A. N. Anagnostopoulos, K. Kokkou and E. K. Polychroniadis, Semicond. Sci. Technol. 13 86-92 (1998)
 [27] J. D. Jensen, J. R. Bruke, D. W. Ernst and R. S. Allgaier, Phys. Rev. B, 6, 319 (1972)
 [28] N. S. Popovich, V. K. Shura, V. P. Daikonov, I. M. Fita and G. G. Levchenko, Sol. Stat. Comm. 50, 979 (1984)
 [29] L. Fu, Phys. Rev. Lett. 103 266801 (2009)

[30] Z. Alpichshev. et al., Phys. Rev. Lett. 104 016410 (2010)